

Activation of p42 Mitogen-activated Protein Kinase (MAPK), but not c-Jun NH₂-Terminal Kinase, Induces Phosphorylation and Stabilization of MAPK Phosphatase XCL100 in *Xenopus* Oocytes

Michael L. Sohaskey*[†] and James E. Ferrell, Jr.

Department of Molecular Pharmacology and Program in Cancer Biology, Stanford University School of Medicine, Stanford, California 94305-5174

Submitted July 9, 2001; November 5, 2001; Accepted November 27, 2001
Monitoring Editor: Marc Mumby

Dual-specificity protein phosphatases are implicated in the direct down-regulation of mitogen-activated protein kinase (MAPK) activity *in vivo*. Accumulating evidence suggests that these phosphatases are components of negative feedback loops that restore MAPK activity to low levels after diverse physiological responses. Limited information exists, however, regarding their post-transcriptional regulation. We cloned two *Xenopus* homologs of the mammalian dual-specificity MAPK phosphatases MKP-1/CL100 and found that overexpression of XCL100 in G2-arrested oocytes delayed or prevented progesterone-induced meiotic maturation. Epitope-tagged XCL100 was phosphorylated on serine during G2 phase, and on serine and threonine in a p42 MAPK-dependent manner during M phase. Threonine phosphorylation mapped to a single residue, threonine 168. Phosphorylation of XCL100 had no measurable effect on its ability to dephosphorylate p42 MAPK. Similarly, mutation of threonine 168 to either valine or glutamate did not significantly alter the binding affinity of a catalytically inactive XCL100 protein for active p42 MAPK *in vivo*. XCL100 was a labile protein in G2-arrested and progesterone-stimulated oocytes; surprisingly, its degradation rate was increased more than twofold after exposure to hyperosmolar sorbitol. In sorbitol-treated oocytes expressing a conditionally active Δ Raf-DD:ER chimera, activation of the p42 MAPK cascade led to phosphorylation of XCL100 and a pronounced decrease in the rate of its degradation. Our results provide mechanistic insight into the regulation of a dual-specificity MAPK phosphatase during meiotic maturation and the adaptation to cellular stress.

INTRODUCTION

Members of the mitogen-activated protein kinase (MAPK) family play fundamental roles in the cellular response to diverse extracellular stimuli, including mitogens, cytokines, and environmental stresses (reviewed by Waskiewicz and Cooper, 1995; Ferrell, 1996; Lewis *et al.*, 1998; Davis, 2000; Pearson *et al.*, 2001). Activation of p42 MAPK and p44 MAPK in quiescent fibroblasts, for example, contributes to the induction of cyclin D expression and entry into the cell

cycle (Pagès *et al.*, 1993; Sun *et al.*, 1994; Brondello *et al.*, 1995; Cheng *et al.*, 1998). Constitutive activation of MAPK cascades can cause cell transformation in fibroblasts (Cowley *et al.*, 1994; Mansour *et al.*, 1994) and, in a context-dependent and MAPK-specific manner, either promote or prevent apoptosis (Xia *et al.*, 1995; Meier and Evan, 1998; Bonni *et al.*, 1999). Thus, from a cellular perspective, precise regulation of MAPK activity can literally signify the difference between life and death.

The meiotic maturation of *Xenopus* oocytes provides an elegant system for studying the biochemistry of p42 MAPK regulation. Activation of the p42 MAPK cascade is important at multiple points during maturation: for the initial activation of Cdc2 triggering the G2-M transition (Sagata *et al.*, 1988; Kosako *et al.*, 1994b, 1996; Gotoh *et al.*, 1995; Palmer *et al.*, 1998); for Cdc2 reactivation and the suppression of DNA replication during the transition from meiosis 1 to meiosis 2 (Furuno *et al.*, 1994); and for the maintenance of

Article published online ahead of print. Mol. Biol. Cell 10.1091/mbc.01-11-0553. Article and publication date are at www.molbiol-cell.org/cgi/doi/10.1091/mbc.01-11-0553.

* Corresponding author. E-mail address: sohaskey@socrates.berkeley.edu.

[†] Present address: University of California, Berkeley, Department of Molecular and Cell Biology, 585 Life Sciences Addition, Berkeley, CA 94720-3200.

metaphase (cytostatic factor) arrest in mature oocytes and eggs (Sagata *et al.*, 1989; Kosako *et al.*, 1994a; Minshull *et al.*, 1994; Abrieu *et al.*, 1996; Cross and Smythe, 1998). In addition, a second MAPK pathway culminating in the activation of c-Jun NH₂-terminal kinase/stress-activated protein kinase (JNK/SAPK) has been discovered recently in *Xenopus* oocytes treated with progesterone or subjected to hyperosmolar stress (Bagowski *et al.*, 2001). It has been hypothesized that this JNK pathway exerts a proapoptotic effect in mature oocytes and early embryos.

MAPKs are activated by the phosphorylation of neighboring threonine and tyrosine residues within a T-X-Y sequence motif located in the activation loop of the kinase domain (Anderson *et al.*, 1990; Payne *et al.*, 1991; Zhang *et al.*, 1994). Both phosphorylations are accomplished by dual-specificity mitogen-activated protein (MAP) kinase kinases, known as MEKs, MAPKKs, or MKKs (Crews *et al.*, 1992; Kosako *et al.*, 1992; Wu *et al.*, 1992). Dual phosphorylation is necessary for full activation of MAPKs, and dephosphorylation of either residue is sufficient for their inactivation (Anderson *et al.*, 1990; Posada and Cooper, 1992; Robbins *et al.*, 1993). Several families of MAPK-directed phosphatases have been identified that can selectively dephosphorylate MAPKs on tyrosine, threonine, or both. Members of the latter group, termed dual-specificity phosphatases, are similar in sequence to the tyrosine phosphatases, and dephosphorylate both residues *in vitro* via a catalytic mechanism analogous to that of tyrosine phosphatases (Ishibashi *et al.*, 1992; Zhou *et al.*, 1994; Denu *et al.*, 1996a,b).

The prototype for the dual-specificity family of MAPK phosphatases is the MAP kinase phosphatase-1 (MKP-1) protein. Mouse MKP-1 and its human homolog, CL100, were originally identified as immediate-early genes that were transcriptionally induced by growth factors, oxidative stress, and heat shock (Charles *et al.*, 1992; Keyse and Emslie, 1992). Both proteins localize to the nucleus in transfected COS-1 cells and exhibit broad substrate specificities for p42/p44 MAPK, JNK/SAPK, and p38/HOG1 (reviewed by Keyse, 1998).

Since the initial identification of MKP-1/CL100, at least nine other distinct MKP family members have been cloned and characterized. The individual MKPs differ slightly with regard to their specificity for different MAPKs, inducibility by extracellular stimuli, and subcellular localization. Expression of most, if not all, of these phosphatases is induced by the same stimuli that induce activation of MAPKs, suggesting that MKPs may be involved in negative feedback loops regulating MAPK activity. In support of this model, Brondello *et al.* (1997) demonstrated that specific activation of the p42/p44 MAPK cascade in CCL39 fibroblasts up-regulates expression of MKP-1 and MKP-2, both of which are absent from quiescent cells.

Despite the ever-increasing number of MKP family members identified to date, little is known about the posttranscriptional mechanisms by which cells regulate MKPs to ensure the appropriate inactivation of distinct MAPKs. We sought to understand the regulation of one particular MKP in our biochemical system of choice, *Xenopus* oocytes. To this end, we cloned two highly similar *Xenopus* MKP-1/CL100 homologs and examined the status of an epitope-tagged XCL100 protein in oocytes exposed to either the maturation-inducing hormone progesterone or the hyperosmolar stress

sorbitol. Whereas progesterone-stimulated oocytes activate both their p42 MAPK and JNK pathways, sorbitol-treated oocytes robustly activate only the JNK pathway (Bagowski *et al.*, 2001). *Xenopus* oocytes therefore provide an attractive system for studying the posttranscriptional regulation of a dual-specificity MAPK phosphatase during the meiotic cell cycle and the adaptive response to hyperosmotic shock.

MATERIALS AND METHODS

Recombinant Proteins, Antibodies, and Other Reagents

The cDNA for a human Raf-1-estrogen receptor chimera, denoted Δ Raf-DD:ER (Bosch *et al.*, 1997), was a generous gift from Martin McMahon (University of California, San Francisco Cancer Center, San Francisco, CA). The Δ Raf-DD:ER cDNA was subcloned into the pSP64(polyA) vector (Promega, Madison, WI) for *in vitro* transcription by Wen Xiong (Stanford University, Stanford, CA). The glutathione S-transferase fusion protein GST-c-Jun (1-79), denoted GST-Jun, was expressed in *Escherichia coli* and purified to homogeneity by glutathione-Sepharose chromatography by Christoph Bagowski (Stanford University) as described (Bagowski *et al.*, 2001). Hexahistidine-tagged *Xenopus* p42 MAPK(K57R) was purified by nickel chelate chromatography (Ferrell and Bhatt, 1997) and phosphorylated with [γ -³²P]ATP as described previously (Sohaskey and Ferrell, 1999). Bisphosphorylated, active murine p42 MAPK and lambda protein phosphatase were obtained from New England Biolabs (Beverly, MA) at specific activities of 5000 and 300 U/ μ g, respectively.

p42 MAPK antiserum DC3 was raised against a carboxy-terminal 12-amino acid peptide from the *Xenopus* p42 MAPK sequence (Hsiao *et al.*, 1994). MEK antiserum 662 was raised in our laboratory as previously described (Hsiao *et al.*, 1994). The polyclonal p90 Rsk (C-21) antibody and the polyclonal estrogen receptor α (HC-20) antibody were obtained from Santa Cruz Biotechnology (Santa Cruz, CA). The monoclonal c-Myc (9E10) antibody was obtained from Babco (Richmond, CA). Alkaline phosphatase-conjugated secondary antibodies were obtained from Sigma (St. Louis, MO).

Progesterone, D-sorbitol, and cycloheximide were obtained from Sigma. ¹²⁵I-labeled protein A and [³²P]orthophosphate were obtained from ICN Pharmaceuticals (Irvine, CA). The MEK inhibitor U0126 (Promega) was reconstituted in dimethyl sulfoxide at a concentration of 10 mM and used at a final concentration of 50 μ M, the lowest concentration that completely and reproducibly prevented p42 MAPK activation in oocytes (our unpublished observations; Gross *et al.*, 2000; Bagowski *et al.*, 2001).

Cloning of XCL100 cDNAs

Total ovary first-strand cDNA (kindly provided by Polly Wong, Stanford University) was used as a template in pairwise polymerase chain reactions (PCRs) with the degenerate oligonucleotides S1 (5'-TG[C/T]CCXAA[C/T]CA[C/T]TT[C/T]GA[A/G]GG-3'), A1 (5'-[C/T]TGXCCCAT[A/G]AA[A/G]CT[A/G]AA[A/G]TT-3'), and A2 (5'-[C/T]TGXCCCAT[A/G]AAXGA[A/G]AA[A/G]TT-3'), where X represents any of the four standard DNA nucleotides. The resulting PCR products were subcloned directly into the TA Cloning vector pCRII (Invitrogen, Carlsbad, CA). To confirm their sequence similarity to mouse MKP-1 and human CL100, individual cDNA clones were sequenced on both strands by the dideoxynucleotide chain-termination method (Sanger *et al.*, 1977), by using reagents and protocols supplied by Amersham Biosciences (Piscataway, NJ). One cDNA clone (designated Xm10) showing high-sequence homology to MKP-1/CL100 was used as a probe in screening a *Xenopus* ovary cDNA library constructed in the Uni-ZAP XR vector (Stratagene, La Jolla, CA).

Approximately 6×10^5 recombinants from this library were screened with a ^{32}P -labeled X_m10 probe following standard protocols (Sambrook *et al.*, 1989). After three rounds of screening, 12 positive clones were plaque purified, and the corresponding cDNA inserts were excised from the Uni-ZAP vector as pBluescript SK(-) phagemids. Partial DNA sequencing of all 12 positive clones separated them into two distinct groups. The longest cDNA from each group was sequenced completely on both strands by the dideoxynucleotide chain-termination method (Sanger *et al.*, 1977). These two clones, 2145 base pairs and 1999 base pairs in length, represented distinct, full-length *Xenopus* MKP-1/CL100 homologs and were renamed XCL100 α and XCL100 β , respectively. EMBL/GenBank/DBJ accession numbers are AJ320158 (XCL100 α) and AJ320159 (XCL100 β).

The predicted XCL100 α and XCL100 β protein sequences were analyzed for PEST regions by using the PESTfind Analysis program, available on the European Molecular Biology Network server at <http://emb1.bcc.univie.ac.at/embnet/tools/bio/PESTfind>. Consensus phosphorylation sites for the cAMP-dependent protein kinase (PKA) were predicted using PhosphoBase v2.0 (Kreegipuu *et al.*, 1999), available on the Center for Biological Sequence Analysis database server at <http://www.cbs.dtu.dk/databases/PhosphoBase/predict/predict.html>.

Subcloning and Epitope Tagging of XCL100

The 10-residue c-Myc epitope EQKLISEEDL was introduced at the carboxy terminus of XCL100 as follows. A 185-base pair fragment containing the carboxy-terminal 146 base pairs of the XCL100 coding region followed by the Myc epitope and an in-frame stop codon was generated by PCR with the primers MKPmycA1 (5'-GAGAGACTGCAGTCACAAGTCTCTCAGAAATGAGCTTTT-GCTCGAGGCAGCTTGGTGATGTAGT-3') and S2 (5'-CAGAAG-CAGGTAGCCCTA-3'). The MKPmycA1 primer introduced an *Xho*I site between the XCL100 coding sequence and the Myc epitope, as well as a *Pst*I site immediately downstream of the stop codon. This PCR product was digested with *Xba*I and *Pst*I to generate a fragment of ~160 base pairs. The XCL100 α cDNA in the pBluescript SK(-) vector was digested with *Hind*III and *Xba*I to obtain a 1.08-kb *Hind*III-*Xba*I fragment that was ligated to the *Xba*I-*Pst*I digested PCR product, yielding an ~1.24-kb *Hind*III-*Pst*I fragment containing the entire XCL100 open reading frame (plus 89 base pairs of the 5'-untranslated region) upstream of the carboxy-terminal Myc epitope.

The ~1.24-kb *Hind*III-*Pst*I XCL100 fragment was then ligated into the *Hind*III-*Pst*I digested pSP64(polyA) vector to yield pSP64myc-XCL100. The fidelity of PCR was established by DNA sequencing.

Site-directed Mutagenesis of XCL100

Site-directed mutagenesis of the XCL100 cDNA was performed using the MORPH site-specific plasmid DNA mutagenesis kit (Eppendorf-5 Prime, Boulder, CO) following the manufacturer's protocol. The mutagenic oligonucleotides used were: C260S (5'-GG-GATATACCAGCTTGGCTGTGGA CAAACACCC-3'), used to mutate cysteine 260 to serine; T168E (5'-CCCTGT GGAGAGC-CACTCTAT-3'), used to mutate threonine 168 to glutamate; and T168V (5'-CCCTGTGGAGTTCCACTCTAT-3'), used to mutate threonine 168 to valine. The fidelity of all mutagenesis procedures was verified by DNA sequencing.

Isolation of *Xenopus* Oocytes and Induction of Maturation

X. laevis females were primed by injection of 50–67 IU of pregnant mare serum gonadotropin (Calbiochem) 3–30 d before oocyte removal. Stage VI oocytes, isolated and maintained as previously described (Sohaskey and Ferrell, 1999), were induced to reenter meiosis 1 and undergo germinal vesicle breakdown (GVBD) by

treatment with 5 $\mu\text{g}/\text{ml}$ progesterone. GVBD was scored by the appearance of a white spot at the animal pole of the oocyte.

Oocyte Microinjections

For expression of Myc-tagged XCL100 proteins in stage VI oocytes, the appropriate pSP64myc-XCL100 DNA was first linearized with *Pvu*II. Capped, polyadenylated mRNA was then transcribed in vitro from this template by using the mMMESSAGE mMACHINE SP6 kit (Ambion, Austin, TX) according to the manufacturer's instructions, purified by phenol/chloroform extraction and isopropanol precipitation, and resuspended in diethylpyrocarbonate-treated water at 1 mg/ml. In vitro-transcribed mRNA was microinjected into the cytoplasm of stage VI oocytes, and injected oocytes were incubated in OR2 buffer (82.5 mM NaCl, 2.5 mM KCl, 1 mM CaCl₂, 1 mM Na₂HPO₄, 5 mM HEPES, pH 7.5) to allow protein expression. Oocytes were collected, frozen on dry ice, and stored at -80°C .

Oocyte Lysis

Oocytes were thawed rapidly and lysed by trituration in ice-cold extraction buffer (EB: 0.25 M sucrose, 0.1 M NaCl, 2.5 mM MgCl₂, 20 mM HEPES, pH 7.2) containing 10 mM EDTA, protease inhibitors (10 $\mu\text{g}/\text{ml}$ leupeptin, 10 $\mu\text{g}/\text{ml}$ pepstatin, 10 $\mu\text{g}/\text{ml}$ aprotinin, 1 mM phenylmethylsulfonyl fluoride), and phosphatase inhibitors (50 mM β -glycerophosphate, 1 mM sodium orthovanadate, 2 μM microcystin), where appropriate. Samples were clarified by centrifugation for 5 min in a Beckman E microcentrifuge (Fullerton, CA) with a right angle rotor. Crude cytoplasm was removed and immediately added to 0.2 volumes of 6 \times Laemmli sample buffer for subsequent SDS-PAGE, or diluted 1:2 in EB/0.2% Triton X-100 plus inhibitors for immunoprecipitation.

SDS-PAGE and Immunoblotting

Samples were separated on 10% SDS polyacrylamide gels (acrylamide:bisacrylamide, 100:1), and the proteins were transferred to an Immobilon P (Millipore, Bedford, MA) blotting membrane. The membrane was blocked with 3% nonfat milk in Tris-buffered saline (150 mM NaCl, 20 mM Tris, pH 7.6) and incubated with primary antibody at a dilution of 1:500 (p42 MAPK and MEK) or 1:1000 (c-Myc, p90 Rsk, and estrogen receptor) for 1–2 h at room temperature. Blots were washed five times with Tris-buffered saline/0.05% Tween 20 and probed with either ^{125}I -labeled protein A for autoradiography, or an alkaline phosphatase-conjugated secondary antibody for detection by enhanced chemiluminescence (ECL) (Amersham Biosciences). For reprobing, blots were stripped by incubation with 100 mM Tris-HCl, pH 7.4, 100 mM 2-mercaptoethanol, and 2% SDS at 70°C for 40 min.

Histone H1 and GST-Jun Kinase Assays

To determine Cdc2 activity, we performed kinase assays with histone H1 as a substrate. Oocytes were lysed in ice-cold EB plus inhibitors (20 $\mu\text{l}/\text{oocyte}$) and clarified in a Beckman E microcentrifuge for 5 min. Three oocyte equivalents were removed from the cytoplasmic fraction, diluted 1:2 in immunoprecipitation buffer (IPB: 15 mM EGTA, 10 mM MgCl₂, 25 mM Tris, pH 8.0, 0.1% Triton X-100, 0.1% bovine serum albumin) plus protease and phosphatase inhibitors, mixed with 18 μl of p13 Suc1 agarose, and incubated at 4°C for 3 h with rocking. After three washes with ice-cold immunoprecipitation buffer plus inhibitors, H1 kinase buffer (0.4 mM ATP, 0.25 $\mu\text{Ci}/\mu\text{l}$ [γ - ^{32}P]ATP, 0.5 mg/ml histone H1, 30 mM 3-(*N*-morpholino)propanesulfonic acid, pH 7.2, 7.5 mM MgCl₂, 0.3 mM dithiothreitol) was added to the beads, yielding a final reaction volume of ~30 μl . The reactions were incubated at 30°C for 10 min and stopped by the addition of 0.2 volumes of 6 \times Laemmli sample buffer. Proteins were electrophoresed on 12.5% SDS polyacrylamide gels (acrylamide:bisacrylamide, 29:1), transferred to Immobilon P

(Millipore) blotting membranes, and ^{32}P -labeled histone H1 was visualized by autoradiography.

To determine JNK activity, GST-Jun kinase assays were performed as described previously (Bagowski *et al.*, 2001) and quantified with a Molecular Dynamics (Sunnyvale, CA) PhosphorImager.

XCL100 Immunoprecipitation and Immunocomplex Phosphatase Assays

For the experiment described in Figure 5A, lysates were prepared immediately after collection of G2- and M-phase oocytes expressing XCL100. Ten oocyte equivalents were diluted 1:1 in EB containing 0.2% Triton X-100 and added to 15 μl of washed protein A-agarose prebound to c-Myc antibody 9E10. After rotation for 2 h at 4°C, immunoprecipitates were washed twice with EB lacking phosphatase inhibitors and once with phosphatase buffer (40 mM HEPES, pH 7.5, 2 mM dithiothreitol, 0.1 mg/ml bovine serum albumin). Ten microliters of 2 \times phosphatase buffer was added together with 10 μl of either buffer or ^{32}P -labeled, bisphosphorylated His₆-p42 MAPK(K57R) (~200 nM final). Reactions were incubated at 30°C for 30 min with occasional gentle mixing and stopped by the addition of 0.2 volumes of 6 \times Laemmli sample buffer. Proteins were resolved by electrophoresis on 10% SDS polyacrylamide gels (acrylamide:bisacrylamide, 100:1) and transferred to Immobilon P (Millipore) blotting membranes. The loss of radiolabel in p42 MAPK(K57R) over time was visualized by autoradiography, quantified with a Molecular Dynamics PhosphorImager, and normalized to the radiolabel remaining in a control sample containing ^{32}P -labeled p42 MAPK(K57R) alone. Immunoprecipitated XCL100 proteins were analyzed by 9E10 immunoblotting.

Phosphoamino Acid Analysis

^{32}P -labeled XCL100 proteins were excised from blotting membranes and subjected to two-dimensional phosphoamino acid analysis at pH 1.9 in the first dimension and pH 3.5 in the second dimension (Boyle *et al.*, 1991; Kamps, 1991). Radiolabeled XCL100 proteins and their constituent phosphoamino acids were visualized by autoradiography.

Data Quantification and Curve Fitting

To quantify XCL100 degradation (Figures 6 and 7), ECL-based densitometry was done using the Kodak Image Station 440CF and 1D Image Analysis Software (Eastman Kodak Company, New Haven, CT). Appropriate controls were evaluated to ensure that all data analyses were performed within the linear range of the system.

To generate the curves shown in Figures 6B and 7, and to estimate half-lives for XCL100, we fit the experimental degradation data to the equation % XCL100 remaining = $100 \times (0.05)^{t/\tau}$ by using KaleidaGraph (Abelbeck Software, Reading, PA). τ represents the half-life of XCL100, and $\ln 2/\tau$ is the apparent zero order rate constant for the degradation reaction.

RESULTS

Cloning of Two Xenopus Homologs of MAPK Phosphatase MKP-1/CL100

As the first step in studying the regulation of a dual-specificity p42 MAPK phosphatase during the meiotic cell cycle, we cloned the *Xenopus* homolog of the murine/human dual-specificity phosphatases MKP-1/CL100. Using degenerate oligonucleotides derived from two carboxy-terminal stretches invariably conserved among the MKP family members MKP-1, CL100, and PAC-1 (Rohan *et al.*, 1993), we performed PCR and amplified a single fragment of the predicted size from a template of stage VI oocyte first-strand

cDNA. Screening an ovary cDNA library with this partial fragment yielded two highly similar yet distinct groups of sequences (our unpublished observations). These sequences are, on average, 77% identical in their predicted protein sequence to MKP-1 and CL100, including 100% identity within the canonical phosphatase catalytic domain (VHC-QAGISRS). Moreover, the two sequences are 94% identical to each other, suggesting that they correspond to pseudoalloploid alleles, a common manifestation of the tetraploid ancestry of *X. laevis* (Jones *et al.*, 1988). For this reason, we named these clones XCL100 α and XCL100 β . The longest XCL100 α and XCL100 β cDNAs isolated were 2145 and 1999 base pairs in length, respectively, and represent full-length XCL100 sequences. Both cDNAs encode proteins of 369 amino acids (apparent molecular mass ~40 kDa) and contain termination codons upstream of and in-frame with the initiation codon ATG. Each cDNA also possesses, within its 3'-untranslated region, three copies of the mRNA destabilization sequence AUUUA (Shaw and Kamen, 1986) (our unpublished observations). The presence of AUUUA sequences is consistent with the finding that XCL100 mRNA levels decrease dramatically coincident with the first cleavage division in the fertilized egg (Lewis *et al.*, 1995). We chose to concentrate our studies on XCL100 α , which corresponds to the XCL100 sequence isolated by Lewis *et al.* (1995).

Coupled transcription/translation of this XCL100 cDNA in a rabbit reticulocyte lysate yielded one prominent band of ~40 kDa (our unpublished observations). In addition, a GST-XCL100 fusion protein selectively dephosphorylated *Xenopus* p42 MAPK on both tyrosine and threonine residues in a time-dependent manner in vitro (Wang *et al.*, 1997; our unpublished observations). Phosphatase activity was prevented by the inclusion of the tyrosine phosphatase inhibitor sodium orthovanadate and was absent in a GST-XCL100(C260S) fusion protein having its essential catalytic cysteine residue mutated to serine. These data support the identity of XCL100 as a dual-specificity p42 MAPK-directed phosphatase.

The expression levels of the endogenous XCL100 protein are relatively low in G2- and M-phase oocytes (Lewis *et al.*, 1995). Therefore, we have used an epitope-tagged XCL100 protein as a surrogate for the endogenous phosphatase in our experiments.

Overexpression of XCL100 Prevents Progesterone-induced Oocyte Maturation

Having established its activity as a p42 MAPK phosphatase in vitro, we next asked whether XCL100 could function as a p42 MAPK-inactivating protein in vivo. To do this, we exploited the ability of fully grown *Xenopus* oocytes to undergo maturation in response to progesterone treatment. Several groups have reported a requirement for activation of the p42 MAPK cascade in progesterone-induced maturation (Sagata *et al.*, 1988; Kosako *et al.*, 1994b; Gotoh *et al.*, 1995). We reasoned that if p42 MAPK activity were indeed important for this process then overexpression of XCL100 in oocytes should prevent p42 MAPK activation and inhibit meiotic progression.

We microinjected in vitro-transcribed mRNA encoding a Myc-tagged version of either wild-type or catalytically inactive (C260S) XCL100 protein into immature stage VI oocytes,

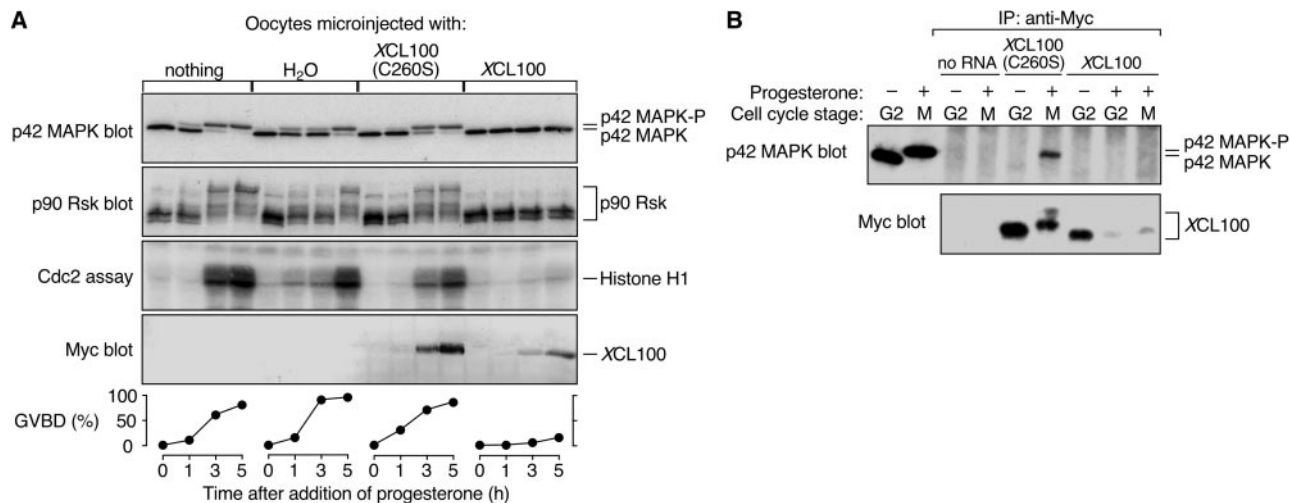


Figure 1. XCL100 functions as a p42 MAPK phosphatase in oocytes. (A) Overexpressed XCL100 prevents progesterone-induced meiotic maturation. Stage VI oocytes were microinjected with either water or mRNA (50 ng) encoding Myc-tagged XCL100 or XCL100(C260S), and incubated briefly to initiate protein expression. GVBD and activation of p42 MAPK, p90 Rsk, and Cdc2 were monitored at various times after the addition of progesterone (5 μ g/ml). Activation of p42 MAPK and p90 Rsk was assessed by immunoblotting, Cdc2 activation was assessed by histone H1-directed kinase activity in p13 Suc1-agarose precipitates, and GVBD was scored by the appearance of a white spot at the animal pole of the oocyte. Expression of Myc-tagged XCL100 proteins was assessed by immunoblotting with the Myc antibody 9E10. (B) XCL100(C260S) forms a stable complex with active p42 MAPK in vivo. G2- and M-phase oocytes (10 per sample) expressing XCL100 or XCL100(C260S) were lysed and subjected to immunoprecipitation with 9E10. Half of each sample was immunoblotted with the p42 MAPK antiserum DC3, and the other half was immunoblotted with 9E10 to detect XCL100 proteins. The first two lanes of the p42 MAPK blot represent uninjected oocytes (one per lane) incubated with (+) or without (-) 5 μ g/ml progesterone as controls for active and inactive p42 MAPK, respectively. Cell cycle stage was determined by the presence (M) or absence (G2) of GVBD. p42 MAPK-P, phosphorylated, active p42 MAPK.

which were subsequently incubated with progesterone to promote cell cycle reentry. Successful maturation was scored visually by GVBD, the appearance of a white spot at the animal pole of the oocyte. Meiotic progression was monitored biochemically by examining the activation state of several key M-phase protein kinases, including p42 MAPK, the p42 MAPK substrate p90 Rsk, and Cdc2/cyclin B. As shown in Figure 1A, overexpression of XCL100 strongly inhibited meiotic progression in progesterone-treated oocytes, whereas oocytes injected with either water alone or XCL100(C260S) mRNA matured with normal kinetics. Interestingly, activation of MEK, the relevant mitogen-activated protein kinase in *Xenopus* oocytes, was also blocked in XCL100-injected oocytes (our unpublished observations). This latter finding further supports the existence of a positive feedback loop operating within the p42 MAPK cascade (Gotoh *et al.*, 1995; Matten *et al.*, 1996; Roy *et al.*, 1996; Howard *et al.*, 1999).

Immunoprecipitation of the XCL100 and XCL100(C260S) proteins from G2- and M-phase oocytes demonstrated that XCL100(C260S) stably binds only the bisphosphorylated, active form of p42 MAPK (Figure 1B). XCL100(C260S) thus acts as a "substrate trap" (Sun *et al.*, 1993), forming a stable complex with its putative substrate, active p42 MAPK. The expression levels of XCL100 protein were markedly lower in M-phase oocytes than in G2-phase oocytes (Figure 1B), suggesting that the phosphatase may be degraded in a progesterone-dependent manner (see below). Significantly, neither MEK, nor p90 Rsk, nor Cdc2/cyclin B were dephosphorylated by XCL100 in vitro (Huang, Sohaskey, and Ferrell,

unpublished observations) or in *Xenopus* oocyte extracts (Alessi *et al.*, 1993). Together, these results suggest that overexpressed XCL100 blocks progesterone-stimulated meiotic maturation by directly dephosphorylating and inactivating p42 MAPK or a p42 MAPK-related protein, such as JNK.

Although overexpressed XCL100 strongly inhibits maturation, we consistently observed GVBD in a subpopulation (typically 10–20%) of oocytes injected with XCL100 mRNA (Figure 1A, bottom). Moreover, none of these GVBD-positive oocytes contained detectable levels of active p42 MAPK by immunoblot analysis (our unpublished observations). These data support three other groups' findings that p42 MAPK activation, despite its proposed role in facilitating an unperturbed meiotic cell cycle, may be dispensable for progression into meiosis 1 in some oocytes (Fabian *et al.*, 1993; Fisher *et al.*, 1999; Gross *et al.*, 2000).

Cell Cycle-dependent Phosphorylation of XCL100

Another intriguing observation to arise from these results concerns the reduced mobility of the XCL100(C260S) protein in mature oocytes (Figures 1B and 2A). Because phosphorylation is a frequently exploited mechanism for signal transduction in eukaryotic cells (Hunter, 1995), we investigated whether the progesterone-dependent mobility shift of XCL100(C260S) was attributable to phosphorylation. Lysates from mature oocytes expressing XCL100(C260S) were treated with lambda protein phosphatase (λ PP), a nonspecific protein phosphatase, and analyzed by SDS-PAGE and immunoblotting. Treatment with λ PP caused the more

slowly migrating forms of XCL100(C260S) to collapse down into a single band, an effect that was prevented by the inclusion of millimolar concentrations of the phosphatase inhibitors sodium orthovanadate and sodium fluoride (Figure 2B). Surprisingly, the single band resulting from λ PP treatment migrated more rapidly than that seen in untreated G2 lysates, suggesting that XCL100(C260S) may also be phosphorylated in G2-arrested oocytes.

To test this hypothesis and as further verification of these findings, we labeled XCL100- and XCL100(C260S)-injected oocytes with [³²P]orthophosphate in the absence or presence of progesterone. The Myc-tagged proteins were then immunoprecipitated and analyzed by autoradiography. Figure 2C confirms that both XCL100 proteins were phosphorylated in response to progesterone treatment; again, the more slowly migrating forms of XCL100(C260S) were apparent. In addition, XCL100(C260S), and to a lesser extent XCL100, were phosphorylated in G2-arrested oocytes, as suggested by the above-mentioned experiments with λ PP (Figure 2B).

To identify the residue(s) phosphorylated within XCL100, we excised the radiolabeled XCL100 bands and performed phosphoamino acid analysis. Excised proteins were subjected to acid hydrolysis followed by two-dimensional thin-layer electrophoresis. The results (Figure 2D) demonstrate that in G2-phase oocytes, both XCL100 and XCL100(C260S) were phosphorylated on one or more serine residues; in response to progesterone, an additional spot of threonine phosphorylation appeared in each sample. The phosphothreonine present in these samples was not due to contamination from coimmunoprecipitating p42 MAPK (our unpublished observations). Thus, XCL100 is differentially phosphorylated in the presence and absence of progesterone, on one or more serine residues during G2 phase, and on both serine and threonine during M phase.

XCL100 Phosphorylation Requires p42 MAPK Activity

Presuming that the only intrinsic difference between the XCL100 and XCL100(C260S) proteins is their catalytic activity, these results suggested two main possibilities: either XCL100 undergoes autodephosphorylation, or the M-phase phosphorylation of XCL100 is a p42 MAPK-dependent process. To further investigate the latter possibility, we examined whether XCL100 phosphorylation parallels that of p42 MAPK in vivo. If XCL100 phosphorylation were continuously dependent on p42 MAPK activity throughout meiosis, for example, then dephosphorylation of the phosphatase would be predicted at approximately the same time as p42 MAPK inactivation in fertilized eggs. To circumvent the severe cell cycle-inhibitory effect and apparent instability of overexpressed XCL100 in progesterone-treated oocytes (Figures 1 and 2A), XCL100(C260S) was used in the following experiments. Oocytes microinjected with XCL100(C260S) mRNA were incubated with progesterone overnight, thereby allowing the oocytes to complete maturation and arrest the cell cycle at metaphase of meiosis 2 (cytostatic factor arrest). Mature oocytes were then incubated with the calcium ionophore A23187 to simulate fertilization (Sohaskey and Ferrell, 1999), and samples were collected at various times for analysis by SDS-PAGE and immunoblotting.

In A23187-treated oocytes, XCL100(C260S) phosphorylation and p42 MAPK activation persisted for 30–45 min, at

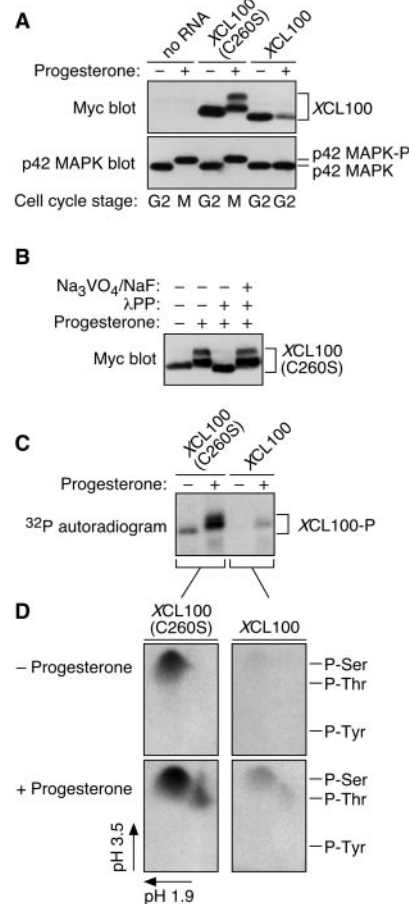


Figure 2. Cell cycle-regulated phosphorylation of XCL100. (A) Lysates from unstimulated and progesterone-stimulated oocytes expressing Myc-tagged XCL100 or XCL100(C260S) were immunoblotted with 9E10 (to detect XCL100 proteins) or DC3 (to detect p42 MAPK) followed by ECL. (B) Lambda protein phosphatase treatment of XCL100(C260S) from mature oocytes. Lysates from XCL100(C260S)-expressing oocytes were treated with (+) or without (-) lambda protein phosphatase (2 U/ μ l for 30 min then an additional 2 U/ μ l for 60 min) in the absence (-) or presence (+) of sodium orthovanadate (Na₃VO₄, 2 mM final) and sodium fluoride (NaF, 10 mM final). XCL100(C260S) proteins were visualized by 9E10 immunoblotting and ECL. (C) Radiolabeling of XCL100 in vivo. Stage VI oocytes, microinjected with mRNA (50 ng) encoding XCL100 or XCL100(C260S), were immediately transferred to phosphate-free OR2 containing 1 mCi/ml [³²P]orthophosphate and incubated 3 h later with (+) or without (-) progesterone. Oocytes (10 per sample) were washed and collected after 7 h, and the radiolabeled XCL100 proteins were immunoprecipitated with 9E10 and visualized by autoradiography. Total radiolabel incorporation was comparable in all sets of oocytes (our unpublished observations). (D) Phosphoamino acid analysis of ³²P-labeled XCL100. The radiolabeled, immunoprecipitated XCL100 proteins were excised from the blotting membrane, subjected to partial acid hydrolysis, and analyzed by two-dimensional thin-layer electrophoresis at pH 1.9 in the first dimension and pH 3.5 in the second dimension. The radiolabeled amino acids were visualized by autoradiography, and their identities were confirmed by comparison to ninhydrin-stained standards (indicated on the right). XCL100-P, phosphorylated XCL100.

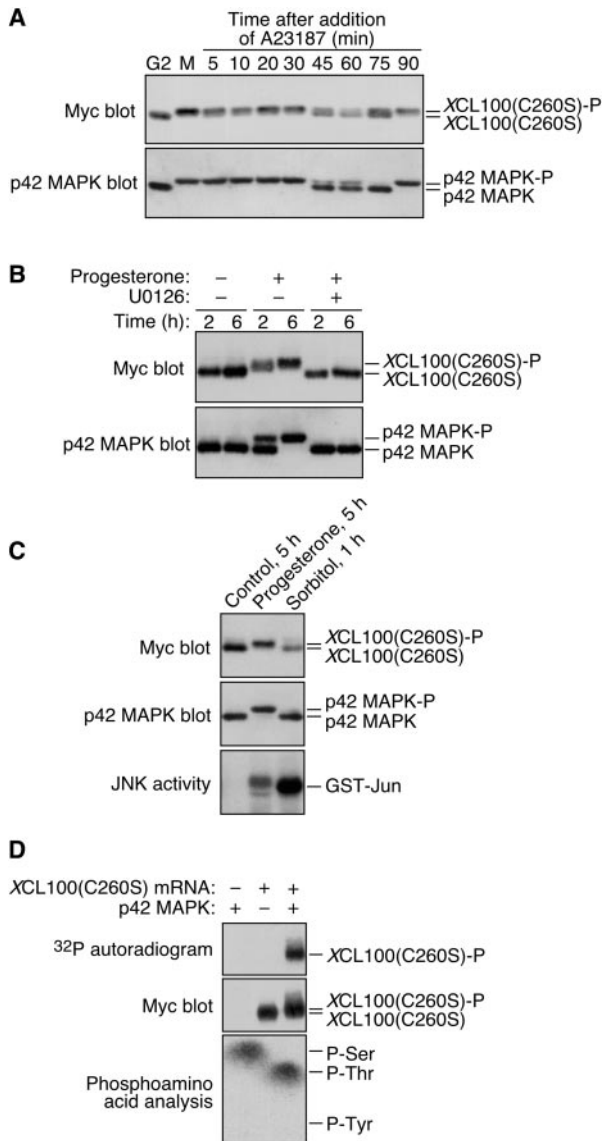


Figure 3. M-phase phosphorylation of XCL100(C260S) is p42 MAPK dependent. (A) XCL100(C260S) phosphorylation parallels that of p42 MAPK throughout meiosis. Stage VI oocytes were microinjected with mRNA (41 ng) encoding Myc-tagged XCL100(C260S) and incubated overnight in the presence or absence of 5 μ g/ml progesterone. The next day, immature (G2) oocytes were collected immediately; mature oocytes (M) were transferred to OR2 containing 5 μ M A23187, and collected at the indicated times. XCL100(C260S) was detected by 9E10 immunoblotting, after which blots were stripped and reprobed with DC3 to detect p42 MAPK. (B) Inhibition of MEK prevents progesterone-induced XCL100(C260S) phosphorylation. Stage VI oocytes expressing XCL100(C260S) were pretreated for 2 h with 50 μ M U0126 or an equal volume of dimethyl sulfoxide (0.5%) as a control. Oocytes were then left unstimulated (-) or stimulated with (+) 5 μ g/ml progesterone, and samples were collected at the indicated times after progesterone treatment (GVBD₅₀ of ~2.5 h). XCL100(C260S) was detected by 9E10 immunoblotting, and p42 MAPK was detected by DC3 immunoblotting. U0126 completely blocked progesterone-induced GVBD in this experiment. (C) Hyperosmolar stress neither activates p42 MAPK nor brings about XCL100(C260S) phosphorylation. Stage VI oocytes

which time both proteins shifted to their more rapidly migrating, dephosphorylated forms (Figure 3A). The highly phosphorylated form of XCL100(C260S) reappeared between 75 and 90 min, concomitant with the reactivation of p42 MAPK. Reactivation of p42 MAPK in these oocytes may reflect the restoration of metaphase arrest triggered by incompletely degraded Mos protein, analogous to the arrest induced by microinjection of Mos into cleaving blastomeres (Sagata *et al.*, 1989). Thus, the phosphorylation state of XCL100(C260S), and presumably by extension that of endogenous XCL100, largely correlates with the activation state of p42 MAPK throughout the meiotic cell cycle.

To determine whether p42 MAPK activation is necessary for XCL100(C260S) phosphorylation, we exploited the pharmacological MEK inhibitor U0126 to block p42 MAPK activation in oocytes expressing the catalytically inactive phosphatase (Favata *et al.*, 1998). As shown in Figure 3B, XCL100(C260S) was quantitatively phosphorylated in response to progesterone treatment, an effect that was completely abrogated by the inclusion of 50 μ M U0126. Significantly, no phosphorylation of XCL100(C260S) was detected in the presence of U0126 despite an approximately sevenfold activation of the MAPK family member JNK in these oocytes (our unpublished observations; Bagowski *et al.*, 2001). Thus, U0126 treatment prevents p42 MAPK activation in oocytes while having little or no effect on JNK activation. Notably, p42 MAPK and JNK are the only MAPK family members known to be activated during *Xenopus* oocyte maturation, further suggesting that the observed effects of U0126 are attributable to its specific inhibition of the p42 MAPK cascade.

To confirm and extend these findings, we subjected XCL100(C260S)-injected oocytes to hyperosmolar stress by exposure to sorbitol, which activates JNK but not p42 MAPK (Bagowski *et al.*, 2001). Consistent with the coincidence of p42 MAPK activation and XCL100 phosphorylation observed in previous experiments, neither p42 MAPK nor XCL100(C260S) was phosphorylated in oocytes incubated in 0.2 M sorbitol for 1 h, by which time JNK was robustly activated (Figure 3C). These data suggest that activation of p42 MAPK, but not the closely related MAPK family member JNK, is required for XCL100 phosphorylation in oocytes.

To address the question of whether p42 MAPK directly phosphorylates XCL100 in oocytes, we tested the ability of recombinant p42 MAPK to phosphorylate XCL100(C260S) in vitro by using XCL100(C260S) expressed in and immuno-

expressing XCL100(C260S) were left unstimulated for 5 h, stimulated with 5 μ g/ml progesterone for 5 h (GVBD₅₀ of ~3.5 h), or treated with 0.2 M sorbitol for 1 h. XCL100(C260S) and p42 MAPK were detected by immunoblotting with 9E10 (top) and DC3 (middle), respectively. JNK activity assays (five oocytes per sample) were performed as described (Bagowski *et al.*, 2001), and phosphorylated GST-Jun was visualized by autoradiography (bottom). (D) p42 MAPK phosphorylates XCL100(C260S) on serine and threonine in vitro. Lysates from G2-arrested oocytes expressing XCL100(C260S) were subjected to immunoprecipitation with 9E10. Immunoprecipitates were treated with (+) or without (-) active mouse p42 MAPK (2 U/ μ l) plus [γ -³²P]ATP for 30 min at 30°C and analyzed by autoradiography (top) and 9E10 immunoblotting (middle). Phosphoamino acid analysis of phosphorylated XCL100(C260S) (bottom) was performed as described in Figure 2D. XCL100(C260S)-P, phosphorylated XCL100(C260S).

precipitated from G2-arrested oocytes. Active p42 MAPK phosphorylated XCL100(C260S) on both serine and threonine residues, causing a modest reduction in its electrophoretic mobility (Figure 3D).

Taken together, these results indicate that p42 MAPK activation is a prerequisite for XCL100 phosphorylation at the G2-M transition of the meiotic cell cycle.

Threonine Phosphorylation of XCL100 Maps to Threonine 168

The discovery that threonine phosphorylation of XCL100 is progesterone-inducible suggested that this phosphorylation may play a particularly important role in the regulation of XCL100 function during meiosis. We therefore sought to map the site of threonine phosphorylation within XCL100. Given our observations that XCL100 phosphorylation is a p42 MAPK-dependent process and that p42 MAPK can phosphorylate XCL100 on both serine and threonine in vitro (Figure 3D), we reasoned that p42 MAPK itself may be the kinase responsible for XCL100 threonine phosphorylation. p42 MAPK phosphorylates substrates containing the motif X-X-(Ser/Thr)-Pro, where X represents any neutral or basic amino acid (Clark-Lewis *et al.*, 1991; Gonzalez *et al.*, 1991; Haycock *et al.*, 1992; Corbalan-Garcia *et al.*, 1996). We scanned the predicted protein sequence of XCL100 for p42 MAPK consensus phosphorylation sites and identified six such sites, four SP and two TP sites (our unpublished observations). Notably, the carboxy terminus of XCL100 also contains a Phe-Asn-Phe-Pro (FNFP) sequence motif; this motif has been shown to serve as a docking site through which p42 MAPK binds many of its substrates (Jacobs *et al.*, 1999).

Only one of the two potential sites of p42 MAPK-mediated threonine phosphorylation, corresponding to threonine 168 in the *Xenopus* phosphatase, is invariant across several MKP family members (our unpublished observations). We mutated this threonine to either a nonphosphorylatable valine (T168V) or a potentially phosphomimetic glutamate (T168E) and repeated in vivo labeling experiments to assess the ability of our mutant XCL100 proteins to undergo threonine phosphorylation. Whereas progesterone stimulated the upward mobility shift of the XCL100(C260S) and XCL100(C260S/T168E) proteins on SDS-PAGE, it largely failed to do so for XCL100(C260S/T168V) (Figure 4A). This finding implicates phosphorylation of threonine 168 as a prerequisite for this mobility shift. Moreover, whereas XCL100(C260S) exhibited its characteristic serine and threonine phosphorylation in progesterone-treated oocytes, XCL100(C260S/T168V) and XCL100(C260S/T168E) were each phosphorylated exclusively on serine under identical circumstances (Figure 4B). Comparable results were obtained for the wild-type XCL100 protein (our unpublished observations). Mutation of threonine 168 affected neither the catalytic activity of the phosphatase (our unpublished observations) nor its ability to bind p42 MAPK in vivo (Figure 5B), suggesting that the lack of threonine phosphorylation in these proteins is not attributable to global changes in protein conformation. In addition, the observed reduction in the electrophoretic mobility of the XCL100(C260S/T168E) protein during M phase supports the notion that XCL100 is also phosphorylated on one or more serine residues at the G2-M transition. We conclude from these results that threonine 168

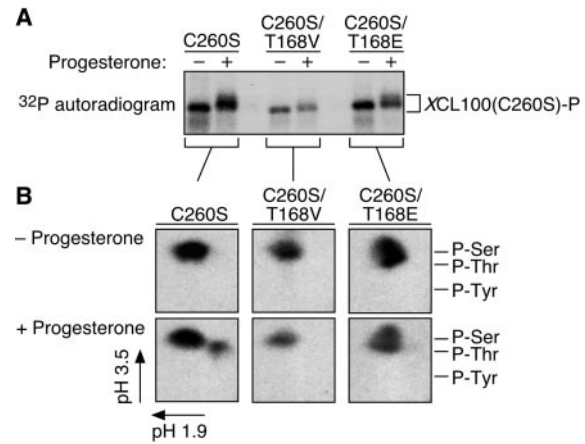


Figure 4. Progesterone-stimulated phosphorylation of XCL100(C260S) on threonine 168. (A) In vivo radiolabeling of XCL100(C260S) proteins mutated at Thr 168. Stage VI oocytes were microinjected with mRNA (50 ng) encoding Myc-tagged XCL100(C260S) or XCL100(C260S) having its threonine 168 residue mutated to valine (T168V) or glutamate (T168E). Oocytes were immediately transferred to phosphate-free OR2 containing 1 mCi/ml [³²P]orthophosphate and processed as described in Figure 2C. (B) Phosphoamino acid analysis of radiolabeled XCL100(C260S) proteins was carried out as detailed in Figure 2D.

represents the lone site of XCL100 threonine phosphorylation in progesterone-stimulated oocytes.

XCL100 Phosphorylation Does not Alter Its Catalytic Activity toward p42 MAPK

Several protein phosphatases, including the dual-specificity phosphatase Cdc25C (Izumi *et al.*, 1992; Kumagai and Dunphy, 1996), undergo a phosphorylation-induced change in catalytic activity. For this reason, we asked whether the progesterone-stimulated, p42 MAPK-dependent phosphorylation of XCL100 served to modulate its phosphatase activity. We found that by titrating the amount of XCL100 mRNA injected per oocyte, we were able to achieve a level of XCL100 expression (at 5 ng of mRNA injected) that was permissive for meiotic maturation (and hence p42 MAPK activation and XCL100 phosphorylation) yet at the same time sufficient for performing immunocomplex phosphatase assays.

Immature, G2-arrested oocytes were microinjected with 5 ng of XCL100 mRNA, incubated in the presence or absence of progesterone, and collected shortly after GVBD₅₀. Myc-tagged XCL100 proteins were then immunoprecipitated, and catalytic activity toward ³²P-labeled *Xenopus* p42 MAPK(K57R) was measured in an immunocomplex phosphatase assay. As shown in Figure 5A (top), XCL100 was highly active toward bisphosphorylated p42 MAPK(K57R) regardless of the cell cycle status of the oocytes from which the protein was isolated. Phosphatase activity was not due to a lack of XCL100 phosphorylation because XCL100 isolated from progesterone-treated oocytes was quantitatively phosphorylated, as indicated by its characteristic mobility shift on SDS-PAGE (Figure 5A,

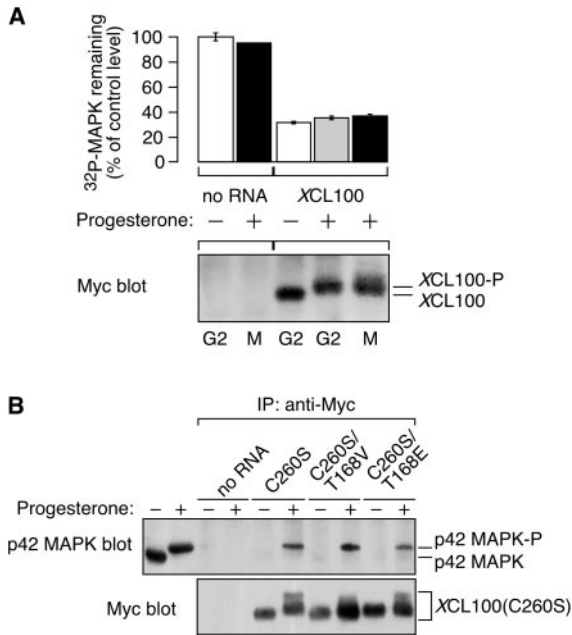


Figure 5. (A) Phosphorylation of XCL100 does not alter its phosphatase activity toward p42 MAPK. Stage VI oocytes were microinjected with mRNA (5 ng) encoding Myc-tagged XCL100 and incubated 2 h later in the absence (-) or presence (+) of 5 μ g/ml progesterone. Oocytes (10 per sample) were collected after 7 h (~GVBD₅₀) and immediately lysed. XCL100 proteins were immunoprecipitated with 9E10, washed extensively, and their activity toward [³²P]p42 MAPK(K57R) was measured in an immunocomplex phosphatase assay (top). Samples were subjected to SDS-PAGE and autoradiography, and ³²P remaining in p42 MAPK(K57R) was quantified and normalized to control [³²P]p42 MAPK(K57R) (represented as 100%). Data are from one experiment with assays performed in duplicate and are shown as averages \pm ranges. Samples processed in parallel, from which the [³²P]p42 MAPK(K57R) had been omitted, were immunoblotted with 9E10 followed by colorimetric detection to visualize the immunoprecipitated XCL100 proteins (bottom). (B) Threonine phosphorylation of XCL100(C260S) does not alter its affinity for active p42 MAPK in vivo. Stage VI oocytes were microinjected with mRNA (46 ng) encoding Myc-tagged XCL100(C260S) or XCL100(C260S) having its threonine 168 mutated to valine (T168V) or glutamate (T168E). Oocytes were processed for immunoprecipitation and immunoblotting as described in Figure 1B. The first two lanes of the p42 MAPK blot represent uninjected oocytes (one per lane) treated with (+) or without (-) 5 μ g/ml progesterone as controls for active and inactive p42 MAPK, respectively.

bottom). No autodephosphorylation of XCL100 was observed in any of these experiments (our unpublished observations). Therefore, our evidence suggests that progesterone-dependent phosphorylation of XCL100 does not significantly alter its catalytic activity toward p42 MAPK.

Threonine Phosphorylation of XCL100 Does not Alter Its Affinity for p42 MAPK

Phosphorylation frequently induces the association or dissociation of enzyme-substrate complexes. Given this prominent role for phosphorylation in influencing protein-pro-

tein interactions, we determined whether progesterone-stimulated phosphorylation of XCL100 on threonine 168 alters the affinity of the phosphatase for p42 MAPK in vivo. We repeated our coimmunoprecipitation experiments from Figure 1B by using the XCL100(C260S/T168V) and XCL100(C260S/T168E) proteins, and immunoblotted for the presence of p42 MAPK in the immunoprecipitates. Comparable amounts of p42 MAPK coprecipitated with each of the XCL100(C260S) proteins from M-phase oocytes, whereas no p42 MAPK was detected in samples from G2-arrested oocytes (Figure 5B). Thus, the phosphorylation state of threonine 168 apparently does not influence the affinity of XCL100 for p42 MAPK in progesterone-treated oocytes. This conclusion is consistent with our finding that mutation of threonine 168 did not affect the potency of XCL100 in preventing GVBD (our unpublished observations). We cannot, however, strictly exclude the possibility that the substrate-trapping capacity of the XCL100(C260S) mutant masks an otherwise inhibitory effect of threonine 168 mutation on p42 MAPK binding.

XCL100 Is a Highly Labile Protein in Sorbitol-treated Oocytes

Previously, we noted that the expression levels of our Myc-tagged XCL100 protein were consistently and dramatically reduced in progesterone-stimulated oocytes relative to unstimulated oocytes (Figures 1B and 2A). This observation suggested that proteolysis may play an important role in regulating the levels of XCL100 during meiosis. Indeed, MKP-1, the murine homolog of XCL100, is a labile protein in mouse (Charles *et al.*, 1992) and hamster (Brondello *et al.*, 1999) fibroblasts, with an estimated half-life of 45 min.

To test the hypothesis that XCL100 is degraded in a progesterone-dependent manner, we treated XCL100-expressing oocytes 7 h after microinjection with progesterone in the presence of the protein synthesis inhibitor cycloheximide. Additionally, as a test of XCL100 stability in response to hyperosmolar stress, we exposed a subset of XCL100-injected oocytes to sorbitol in the presence of cycloheximide. Figure 6 demonstrates that XCL100 was a labile protein in all three sets of oocytes tested. Surprisingly, however, the rate of XCL100 degradation measured in sorbitol-treated oocytes (half-life of ~45 min for $n \geq 6$ experiments) was greater than twice that measured in control and progesterone-stimulated oocytes (half-life of 2–3 h for $n \geq 4$ experiments). Degradation was specific for XCL100 and was not due to cycloheximide-induced cell toxicity, as the levels of endogenous MEK and p42 MAPK remained constant throughout the time course (Figure 6A). The apparent contradiction between the slow rate of progesterone-dependent XCL100 degradation seen in these experiments and the more rapid rate inferred from our previous experiments (Figures 1B and 2A) may be due, in part, to the inhibitory effect of cycloheximide on progesterone-induced maturation in *Xenopus* oocytes (see DISCUSSION). Based on these results, we conclude that hyperosmolar stress up-regulates the proteolysis of an already labile XCL100 protein.

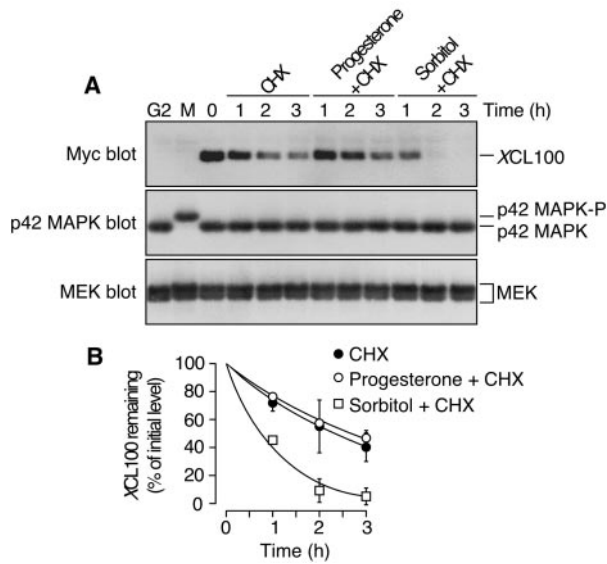


Figure 6. XCL100 is a labile protein in oocytes. (A) stage VI oocytes were microinjected with mRNA (46 ng) encoding Myc-tagged XCL100. Seven hours later, microinjected oocytes were split into three pools and transferred to OR2 containing 50 $\mu\text{g}/\text{ml}$ cycloheximide (CHX) alone, CHX plus 5 $\mu\text{g}/\text{ml}$ progesterone, or CHX plus 0.2 M sorbitol. Samples were collected at the indicated times and immunoblotted with 9E10 (to detect XCL100), DC3 (to detect p42 MAPK), or the MEK antiserum 662. The first two lanes of each blot represent uninjected oocytes treated with (M) or without (G2) 5 $\mu\text{g}/\text{ml}$ progesterone as controls for active and inactive p42 MAPK, respectively. (B) XCL100 proteins were quantified using the Kodak Image Station 440CF and 1D Image Analysis Software. Data are shown as mean values \pm SEM for two independent experiments.

Increased Stability of XCL100 after Its p42 MAPK-dependent Phosphorylation in Sorbitol-treated Oocytes

At least two lines of evidence suggested that p42 MAPK-dependent phosphorylation of XCL100 may lead to a decrease in the rate of its degradation in vivo. First, as documented in Figure 1B, phosphatase-inactive XCL100(C260S) was consistently more stable in progesterone-treated oocytes than was the wild-type phosphatase, coincident with phosphorylation of the XCL100(C260S) protein during M phase. Increased stability of XCL100(C260S) was not attributable to an insensitivity to the cellular degradation machinery because nonphosphorylated XCL100(C260S) was readily degraded in cycloheximide-treated oocytes exposed to sorbitol (our unpublished observations). Second, in oocytes injected with a level of XCL100 mRNA too low to prevent p42 MAPK activation, we immunoprecipitated comparable amounts of phosphorylated and nonphosphorylated XCL100 from M-phase and G2-phase oocytes, respectively (Figure 5A, bottom). These findings implied a decrease in the rate of XCL100 degradation after its phosphorylation.

To investigate this possibility, we exploited an inducible activator of the p42 MAPK cascade, a chimeric protein comprising an oncogenic form of human c-Raf-1 ($\Delta\text{Raf-1 DD}$) fused to the hormone-binding domain of the human estrogen receptor (Bosch *et al.*, 1997). Stage VI oocytes

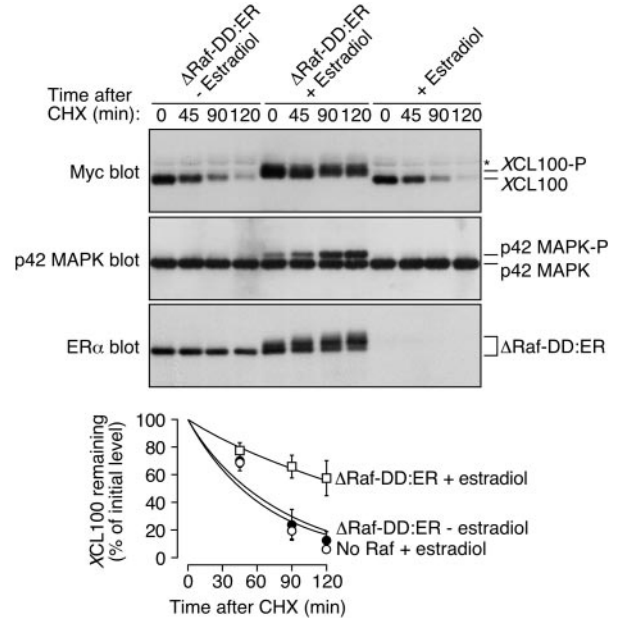


Figure 7. Stabilization of XCL100 follows its p42 MAPK-dependent phosphorylation in sorbitol-treated oocytes. Stage VI oocytes were microinjected with mRNA (46 ng) encoding $\Delta\text{Raf-DD:ER}$ and incubated at 16°C for 8–12 h. Oocytes were then microinjected a second time with mRNA (46 ng) encoding Myc-tagged XCL100 and were split into two pools 4 h later. Estradiol (2 μM) was added to one pool to activate Raf, and an equal volume of ethanol (0.02%) was added to the second pool as a control. Three hours later, oocytes were transferred to OR2 containing 50 $\mu\text{g}/\text{ml}$ cycloheximide (CHX) plus 0.2 M sorbitol. Samples were collected at the indicated times and analyzed by immunoblotting with 9E10 (to detect XCL100), DC3 (to detect p42 MAPK), or an estradiol receptor antibody (to detect $\Delta\text{Raf-DD:ER}$) (top three panels). Oocytes microinjected with XCL100 alone and treated with 2 μM estradiol were processed in parallel as controls to exclude the possibility of nonspecific estradiol-mediated effects. XCL100 proteins were quantified using the Kodak Image Station 440CF and 1D Image Analysis Software (bottom). Data are shown as mean values \pm SEM for three independent experiments. The asterisk to the right of the Myc immunoblot denotes a nonspecific band present in samples from injected and uninjected oocytes.

were microinjected with in vitro-transcribed mRNA encoding this $\Delta\text{Raf-DD:ER}$ protein and incubated overnight before being injected again with XCL100 mRNA. Estradiol (2 μM) was added several hours later to trigger $\Delta\text{Raf-DD:ER}$ kinase activation, after which sorbitol and cycloheximide were added, and XCL100 degradation was assessed by SDS-PAGE and immunoblotting. Figure 7 shows that p42 MAPK activation and XCL100 phosphorylation both followed estradiol treatment of $\Delta\text{Raf-DD:ER}$ -expressing oocytes. Dramatically, the degradation rate of nonphosphorylated XCL100 (half-life of ~ 50 min) was nearly 3 times that of its phosphorylated counterpart (half-life of ~ 145 min). Stabilization of the XCL100 protein was not due to a nonspecific estradiol-mediated effect, because the rate of XCL100 degradation was unaffected by estradiol treatment in oocytes not expressing $\Delta\text{Raf-DD:ER}$.

Collectively, these results indicate a role for p42 MAPK-mediated phosphorylation in stabilizing the XCL100 protein during meiosis

DISCUSSION

Constitutive p42 MAPK activation can have dramatic biological consequences, including inappropriate cell fate changes, cellular senescence (Lin *et al.*, 1998; Zhu *et al.*, 1998), and cellular transformation (Cowley *et al.*, 1994; Mansour *et al.*, 1994). p42 MAPK activity must therefore be tightly controlled throughout the cell cycle to ensure the proper coordination of physiological events. Many dual-specificity phosphatases capable of inactivating MAPK family members *in vivo* have now been cloned and characterized from diverse model organisms. Little is known, however, regarding the mechanisms by which cells restrict the functions of these important proteins. Herein, we reveal one such mechanism for regulating a *Xenopus* MKP-1/CL100 homolog in progesterone- and sorbitol-treated oocytes. Our results elucidate, for the first time, the regulation of a MAPK phosphatase during the meiotic cell cycle and in response to cellular stress.

Stabilization of XCL100 Follows Its p42 MAPK-dependent Phosphorylation

Foremost among our findings is the discovery that stabilization of the normally labile XCL100 protein follows its p42 MAPK-dependent phosphorylation. Two suggestive pieces of evidence emerging from our initial studies prompted us to investigate this possibility directly. First, despite their comparable expression levels in G2-arrested oocytes, levels of wild-type XCL100 were markedly reduced relative to those of catalytically inactive XCL100(C260S) in progesterone-treated oocytes. This difference in expression levels correlated with M-phase phosphorylation of XCL100(C260S) but not XCL100, which in turn correlated with the suppression of progesterone-stimulated p42 MAPK activation by the wild-type phosphatase. Second, similar amounts of non-phosphorylated and phosphorylated XCL100 were isolated from G2-phase and M-phase oocytes, respectively, only when phosphatase expression levels were too low to inhibit p42 MAPK activation and GVBD (Figure 5A). Thus, indirect evidence suggested a cause-and-effect relationship between p42 MAPK-mediated phosphorylation and a decrease in the rate of XCL100 degradation in oocytes.

Direct testing of this hypothesis, however, proved difficult. This difficulty was due to similarly slow rates of XCL100 proteolysis in unstimulated and progesterone-stimulated oocytes treated with cycloheximide to measure protein degradation directly. We suspect that incubation of progesterone-treated oocytes in cycloheximide may have been responsible for the unexpectedly long half-life (2–3 h) of XCL100 under these conditions. Cycloheximide prevents progesterone-induced GVBD and maturation by preventing *de novo* synthesis of key cell cycle proteins such as Mos (Sagata *et al.*, 1988) and Ringo/Speedy (Ferby *et al.*, 1999; Lenormand *et al.*, 1999). By extension, then, cycloheximide would be predicted to impede other events related to meiotic progression, conceivable among them progesterone-dependent activation of one or more components of the protein

degradation machinery. Alternatively, a significant lag time may exist between exposure to progesterone and activation of the degradation machinery.

The ability of sorbitol to induce degradation of the XCL100 protein circumvented this experimental dilemma. Proteolysis of XCL100 in sorbitol-treated oocytes was rapid (half-life of ~45 min) and independent of protein synthesis. A conditionally active Δ Raf-ER:DD protein was used to artificially activate the p42 MAPK cascade and promote XCL100 phosphorylation in these oocytes, allowing the direct measurement of degradation rates for the phosphorylated and nonphosphorylated XCL100 proteins. It should be noted that although XCL100 does not form a stable complex with active p42 MAPK in progesterone-treated oocytes (Figure 1B), our data do not exclude the possibility that transient binding of XCL100 to active p42 MAPK, rather than its p42 MAPK-dependent phosphorylation, induces a conformational change leading to stabilization of the phosphatase. This possibility is analogous to the catalytic activation of MKP family members induced by their direct and selective binding to individual MAPKs (see below).

XCL100 Stabilization Confers Negative Feedback upon p42 MAPK Cascade

In G2-arrested oocytes, XCL100 degradation is slow and appears to be balanced by protein synthesis. Progesterone-triggered activation of the p42 MAPK cascade presumably overwhelms the activity of endogenous XCL100, leading to its p42 MAPK-dependent phosphorylation and stabilization. In contrast, exposure to sorbitol (and possibly other cellular stresses) causes rapid degradation of XCL100 in the absence of significant p42 MAPK activation. Additional work will be needed to determine whether this absence of p42 MAPK activation is due to a lack of cross-talk between the JNK and p42 MAPK pathways in sorbitol-exposed oocytes, or whether instead p42 MAPK activation is actively inhibited under these circumstances.

The fact that p42 MAPK stabilizes its inactivator, XCL100, means that the p42 MAPK/XCL100 system constitutes a negative feedback loop that should tend to moderate or temporally limit the activation of p42 MAPK. Moreover, p42 MAPK may positively regulate XCL100 through at least two other mechanisms: activation of p42 MAPK can induce expression of the closely related phosphatases MKP-1 and MKP-2 (Brondello *et al.*, 1997), and, by analogy to other MKP family members, p42 MAPK may catalytically activate XCL100 by binding to its amino terminus (Camps *et al.*, 1998; Dowd *et al.*, 1998; Fjeld *et al.*, 2000; Chen *et al.*, 2001; Slack *et al.*, 2001). The presence of multiple activation mechanisms may increase the robustness of the p42 MAPK/XCL100 system. Nevertheless, in the oocyte this negative feedback loop appears to be overwhelmed by a stronger positive feedback system (Gotoh *et al.*, 1995; Matten *et al.*, 1996; Roy *et al.*, 1996; Howard *et al.*, 1999; this study) that maintains p42 MAPK activity at high levels despite high levels of phosphatase activity (Sohaskey and Ferrell, 1999).

In contrast, the relationship between XCL100 and its substrate JNK appears to be fundamentally different. Whereas overexpressed XCL100 does prevent JNK activation in oocytes subjected to hyperosmolar stress (our unpublished observations), JNK activation does not suffice to bring about XCL100 phosphorylation and stabilization (Figure 3C).

Thus, the JNK/XCL100 system appears not to constitute a negative feedback loop. Moreover, because sorbitol strongly stimulates both JNK activation and degradation of the phosphatase then either JNK or something upstream of JNK appears to negatively regulate XCL100. This could represent a "double negative" feedback system, with XCL100 and JNK mutually inhibiting each other. Such a system can, in principle, exhibit switch-like bistable behavior, with a stable high JNK/low XCL100 state and a stable low JNK/high XCL100 state, but no stable intermediate states. Indeed, recent work has shown that JNK does exhibit bistable responses in oocytes (Bagowski and Ferrell, 2001). It will be of interest to determine what contribution XCL100 makes to the bistable behavior of JNK.

Meiotic Phosphorylation of XCL100: More than a Stabilizing Influence?

The observed stabilization of XCL100 after its p42 MAPK-dependent phosphorylation in oocytes is consistent with the results of Brondello *et al.* (1999), who found that p42/p44 MAPK-dependent phosphorylation of MKP-1 reduced the rate of its degradation in Chinese hamster lung fibroblast (CCL39) cells. Whereas they identified the sites of p42/p44 MAPK-mediated phosphorylation in MKP-1 as two serine residues exclusively, only one of which is present in the *Xenopus* phosphatase, we have mapped the progesterone-stimulated phosphorylation of XCL100 to one threonine and one or more serines. Moreover, we find that substitution of glutamate for this well-conserved threonine (Thr 168) partially stabilizes XCL100 in response to sorbitol (our unpublished observations). This apparent discrepancy may reflect a legitimate biological difference between different cell types.

Additionally, it is tempting to speculate that threonine phosphorylation may confer an additional level of regulation upon the *Xenopus* phosphatase. In support of this possibility, phosphatase-inactive XCL100(C260S) gel-filters in a high molecular weight complex in G2-arrested oocytes but dissociates from this complex during M phase, concomitant with its progesterone-induced phosphorylation at the G2-M transition (our unpublished observations). It will be important to determine how distinct MKP family members are differentially regulated in diverse biological contexts.

We also noted serine phosphorylation of XCL100 in G2-arrested oocytes. The presence of eight consensus phosphorylation sites for PKA within XCL100 (our unpublished observations), together with the importance of PKA for maintaining oocytes in a G2-like arrest, suggest that phosphorylation by PKA may somehow regulate XCL100 function. Although the physiological relevance of this G2-phase phosphorylation is uncertain, one intriguing possibility arises from recent work by Rafael Pulido's laboratory. This group showed that, in COS-7 cells, the tyrosine phosphatase PTP-SL inactivates and anchors p42 MAPK in the cytoplasm through association of p42 MAPK with a kinase interaction motif (KIM) in PTP-SL (Zúñiga *et al.*, 1999). PKA-catalyzed phosphorylation of Ser 231, located within the KIM, abrogates p42 MAPK binding and favors nuclear translocation of the kinase (Blanco-Aparicio *et al.*, 1999). Future work will seek to determine whether PKA-mediated phosphorylation regulates XCL100 function, perhaps by altering its affinity

for either MAPK family members or the higher molecular weight complex described above.

XCL100 Functions as Both Enzyme and Substrate for p42 MAPK

Despite its ability to fully inactivate both p42 MAPK and JNK (Chu *et al.*, 1996; Hirsch and Stork, 1997; our unpublished observations) *in vivo*, XCL100 appears to be phosphorylated by a strictly p42 MAPK-dependent mechanism. Thus, whereas XCL100 can act as both enzyme and substrate in its relationship with p42 MAPK, the phosphatase acts only as an enzyme in its association with the related MAPK family member JNK. This finding implies that the reciprocal reactions, dephosphorylation of p42 MAPK by XCL100 and phosphorylation of XCL100 by p42 MAPK, are likely mediated by distinct binding events between the two proteins. Consistent with this proposal, we noted the presence of an FNFP motif within the carboxy terminus of XCL100. Jacobs *et al.* (1999) demonstrated that FXFP is an evolutionarily conserved motif that mediates binding of p42 MAPK to various substrate proteins. The discovery that both substrate specificity and tight substrate binding are conferred by the amino terminus of the related phosphatase MKP-3 (Camps *et al.*, 1998; Muda *et al.*, 1998) supports the hypothesis that the FNFP motif within XCL100 mediates its role as a p42 MAPK substrate. In addition, the absence of an analogous experimentally defined JNK docking site (Yang *et al.*, 1998a,b; Jacobs *et al.*, 1999) in XCL100 is consistent with our conclusion that this phosphatase is a poor substrate for JNK.

XCL100 and Protein Degradation Machinery

Brondello *et al.* (1999) showed that MKP-1 degradation proceeds via the ubiquitin-directed proteasome complex. Degradation of XCL100 presumably proceeds via a similar mechanism, although this remains to be formally demonstrated. Moreover, important mechanistic details concerning the targeted degradation of XCL100 and MKP-1 remain a mystery, because neither of these proteins contains any of the recognizable destruction motifs typically found in other labile proteins, including PEST sequences (Rogers *et al.*, 1986), a destruction box (Glutzer *et al.*, 1991), or a KEN box (Pfleger and Kirschner, 2000). Identification of the sequence(s) within XCL100 that direct its ubiquitin-dependent degradation will prove crucial in clarifying the role played by targeted degradation of MKP family members during the meiotic and mitotic cell cycles.

ACKNOWLEDGMENTS

We thank Natalie Ahn, Jonathan Cooper, Martin McMahon, and Jim Posada for providing plasmids; Polly Wong for preparing total ovary first-strand cDNA; Wen Xiong for subcloning the Δ Raf-ER cDNA; Ramesh Bhatt for providing recombinant (His)₆-MEK R4F and (His)₆-p42 MAPK(K57R) proteins; Christoph Bagowski for providing recombinant GST-Jun and for expertise regarding the GST-Jun kinase assay; and Jason Myers, Joe Pomeroy, and Sarah Walter for critical reading of the manuscript. This work was supported by National Institutes of Health grant GM-46383 (to J.E.F.) and a Howard Hughes Medical Institute predoctoral fellowship (to M.L.S.).

REFERENCES

- Abrieu, A., Lorca, T., Labbe, J.C., Morin, N., Keyse, S., and Doree, M. (1996). MAP kinase does not inactivate, but rather prevents the cyclin degradation pathway from being turned on in *Xenopus* egg extracts. *J. Cell Sci.* 109, 239–246.
- Alessi, D.R., Smythe, C., and Keyse, S.M. (1993). The human CL100 gene encodes a Tyr/Thr-protein phosphatase which potently and specifically inactivates MAP kinase and suppresses its activation by oncogenic ras in *Xenopus* oocyte extracts. *Oncogene* 8, 2015–2020.
- Anderson, N.G., Maller, J.L., Tonks, N.K., and Sturgill, T.W. (1990). Requirement for integration of signals from two distinct phosphorylation pathways for activation of MAP kinase. *Nature* 343, 651–653.
- Bagowski, C.P., and Ferrell, J.E., Jr. (2001). Bistability in the JNK cascade. *Curr. Biol.* 11, 1176–1182.
- Bagowski, C.P., Xiong, W., and Ferrell, J.E., Jr. (2001). c-Jun N-terminal kinase activation in *Xenopus laevis* eggs, and embryos. A possible non-genomic role for the JNK signaling pathway. *J. Biol. Chem.* 276, 1459–1465.
- Blanco-Aparicio, C., Torres, J., and Pulido, R. (1999). A novel regulatory mechanism of MAP kinases activation and nuclear translocation mediated by PKA and the PTP-SL tyrosine phosphatase. *J. Cell Biol.* 147, 1129–1136.
- Bonni, A., Brunet, A., West, A.E., Datta, S.R., Takasu, M.A., and Greenberg, M.E. (1999). Cell survival promoted by the Ras-MAPK signaling pathway by transcription-dependent and -independent mechanisms. *Science* 286, 1358–1362.
- Bosch, E., Cherwinski, H., Peterson, D., and McMahon, M. (1997). Mutations of critical amino acids affect the biological and biochemical properties of oncogenic A-Raf and Raf-1. *Oncogene* 15, 1021–1033.
- Boyle, W.J., van der Geer, P., and Hunter, T. (1991). Phosphopeptide mapping and phosphoamino acid analysis by two-dimensional separation on thin-layer cellulose plates. *Methods Enzymol.* 201, 110–149.
- Brondello, J.M., Brunet, A., Pouyssegur, J., and McKenzie, F.R. (1997). The dual specificity mitogen-activated protein kinase phosphatase-1 and -2 are induced by the p42/p44MAPK cascade. *J. Biol. Chem.* 272, 1368–1376.
- Brondello, J.M., McKenzie, F.R., Sun, H., Tonks, N.K., and Pouyssegur, J. (1995). Constitutive MAP kinase phosphatase (MKP-1) expression blocks G1 specific gene transcription and S-phase entry in fibroblasts. *Oncogene* 10, 1895–1904.
- Brondello, J.M., Pouyssegur, J., and McKenzie, F.R. (1999). Reduced MAP kinase phosphatase-1 degradation after p42/p44MAPK-dependent phosphorylation. *Science* 286, 2514–2517.
- Camps, M., Nichols, A., Gillieron, C., Antonsson, B., Muda, M., Chabert, C., Boschert, U., and Arkinstall, S. (1998). Catalytic activation of the phosphatase MKP-3 by ERK2 mitogen-activated protein kinase. *Science* 280, 1262–1265.
- Charles, C.H., Abler, A.S., and Lau, L.F. (1992). cDNA sequence of a growth factor-inducible immediate early gene and characterization of its encoded protein. *Oncogene* 7, 187–190.
- Chen, P., Hutter, D., Yang, X., Gorospe, M., Davis, R.J., and Liu, Y. (2001). Discordance between the binding affinity of mitogen-activated protein kinase subfamily members for MKP-2 and their ability to catalytically activate the phosphatase. *J. Biol. Chem.* 276, 29440–29449.
- Cheng, M., Sexl, V., Sherr, C.J., and Roussel, M.F. (1998). Assembly of cyclin D-dependent kinase and titration of p27Kip1 regulated by mitogen-activated protein kinase kinase (MEK1). *Proc. Natl. Acad. Sci. USA* 95, 1091–1096.
- Chu, Y., Solski, P.A., Khosravi-Far, R., Der, C.J., and Kelly, K. (1996). The mitogen-activated protein kinase phosphatases PAC1, MKP-1, and MKP-2 have unique substrate specificities and reduced activity in vivo toward the ERK2 sevenmaker mutation. *J. Biol. Chem.* 271, 6497–6501.
- Clark-Lewis, I., Sanghera, J.S., and Pelech, S.L. (1991). Definition of a consensus sequence for peptide substrate recognition by p44^{mapk}, the meiosis-activated myelin basic protein kinase. *J. Biol. Chem.* 266, 15180–15184.
- Corbalan-Garcia, S., Yang, S.S., Degenhardt, K.R., and Bar-Sagi, D. (1996). Identification of the mitogen-activated protein kinase phosphorylation sites on human Sos1 that regulate interaction with Grb2. *Mol. Cell. Biol.* 16, 5674–5682.
- Cowley, S., Paterson, H., Kemp, P., and Marshall, C.J. (1994). Activation of MAP kinase kinase is necessary and sufficient for PC12 differentiation and for transformation of NIH 3T3 cells. *Cell* 77, 841–852.
- Crews, C.M., Alessandrini, A., and Erikson, R.L. (1992). The primary structure of MEK, a protein kinase that phosphorylates the ERK gene product. *Science* 258, 478–480.
- Cross, D.A., and Smythe, C. (1998). PD 98059 prevents establishment of the spindle assembly checkpoint and inhibits the G2-M transition in meiotic but not mitotic cell cycles in *Xenopus*. *Exp. Cell Res.* 241, 12–22.
- Davis, R.J. (2000). Signal transduction by the JNK group of MAP kinases. *Cell* 103, 239–252.
- Denu, J.M., Lohse, D.L., Vijayalakshmi, J., Saper, M.A., and Dixon, J.E. (1996a). Visualization of intermediate and transition-state structures in protein-tyrosine phosphatase catalysis. *Proc. Natl. Acad. Sci. USA* 93, 2493–2498.
- Denu, J.M., Stuckey, J.A., Saper, M.A., and Dixon, J.E. (1996b). Form and function in protein dephosphorylation. *Cell* 87, 361–364.
- Dowd, S., Sneddon, A.A., and Keyse, S.M. (1998). Isolation of the human genes encoding the pyst1 and Pyst2 phosphatases: characterization of Pyst2 as a cytosolic dual-specificity MAP kinase phosphatase and its catalytic activation by both MAP and SAP kinases. *J. Cell Sci.* 111, 3389–3399.
- Fabian, J.R., Morrison, D.K., and Daar, I.O. (1993). Requirement for Raf and MAP kinase function during the meiotic maturation of *Xenopus* oocytes. *J. Cell Biol.* 122, 645–652.
- Favata, M.F., et al. (1998). Identification of a novel inhibitor of mitogen-activated protein kinase kinase. *J. Biol. Chem.* 273, 18623–18632.
- Ferby, I., Blazquez, M., Palmer, A., Eritja, R., and Nebreda, A.R. (1999). A novel p34(cdc2)-binding and activating protein that is necessary and sufficient to trigger G(2)/M progression in *Xenopus* oocytes. *Genes Dev.* 13, 2177–2189.
- Ferrell, J.E., Jr. (1996). MAP kinases in mitogenesis and development. *Curr. Top. Dev. Biol.* 33, 1–60.
- Ferrell, J.E., Jr., and Bhatt, R.R. (1997). Mechanistic studies of the dual phosphorylation of mitogen-activated protein kinase. *J. Biol. Chem.* 272, 19008–19016.
- Fisher, D.L., Brassac, T., Galas, S., and Doree, M. (1999). Dissociation of MAP kinase activation and MPF activation in hormone-stimulated maturation of *Xenopus* oocytes. *Development* 126, 4537–4546.
- Fjeld, C.C., Rice, A.E., Kim, Y., Gee, K.R., and Denu, J.M. (2000). Mechanistic basis for catalytic activation of mitogen-activated protein kinase phosphatase 3 by extracellular signal-regulated kinase. *J. Biol. Chem.* 275, 6749–6757.
- Furuno, N., Nishizawa, M., Okazaki, K., Tanaka, H., Iwashita, J., Nakajo, N., Ogawa, Y., and Sagata, N. (1994). Suppression of DNA

- replication via Mos function during meiotic divisions in *Xenopus* oocytes. *EMBO J.* *13*, 2399–2410.
- Glotzer, M., Murray, A.W., and Kirschner, M.W. (1991). Cyclin is degraded by the ubiquitin pathway. *Nature* *349*, 132–138.
- Gonzalez, F.A., Raden, D.L., and Davis, R.J. (1991). Identification of substrate recognition determinants for human ERK1 and ERK2 protein kinases. *J. Biol. Chem.* *266*, 22159–22163.
- Gotoh, Y., Masuyama, N., Dell, K., Shirakabe, K., and Nishida, E. (1995). Initiation of *Xenopus* oocyte maturation by activation of the mitogen-activated protein kinase cascade. *J. Biol. Chem.* *270*, 25898–25904.
- Gross, S.D., Schwab, M.S., Taieb, F.E., Lewellyn, A.L., Qian, Y.W., and Maller, J.L. (2000). The critical role of the MAP kinase pathway in meiosis II in *Xenopus* oocytes is mediated by p90(Rsk). *Curr. Biol.* *10*, 430–438.
- Haycock, J.W., Ahn, N.G., Cobb, M.H., and Krebs, E.G. (1992). ERK1 and ERK2, two microtubule-associated protein 2 kinases, mediate the phosphorylation of tyrosine hydroxylase at serine-31 *in situ*. *Proc. Natl. Acad. Sci. USA* *89*, 2365–2369.
- Hirsch, D.D., and Stork, P.J. (1997). Mitogen-activated protein kinase phosphatases inactivate stress-activated protein kinase pathways *in vivo*. *J. Biol. Chem.* *272*, 4568–4575.
- Howard, E.L., Charlesworth, A., Welk, J., and MacNicol, A.M. (1999). The MAP kinase signaling pathway stimulates Mos mRNA cytoplasmic polyadenylation during *Xenopus* oocyte maturation. *Mol. Cell. Biol.* *19*, 1990–1999.
- Hsiao, K.-M., Chou, S.-Y., Shih, S.-J., and Ferrell, J.E., Jr. (1994). Evidence that inactive p42 mitogen-activated protein kinase and inactive Rsk exist as a heterodimer *in vivo*. *Proc. Natl. Acad. Sci. USA* *91*, 5480–5484.
- Hunter, T. (1995). Protein kinases and phosphatases: the yin and yang of protein phosphorylation and signaling. *Cell* *80*, 225–236.
- Ishibashi, T., Bottaro, D.P., Chan, A., Miki, T., and Aaronson, S.A. (1992). Expression cloning of a human dual-specificity phosphatase. *Proc. Natl. Acad. Sci. USA* *89*, 12170–12174.
- Izumi, T., Walker, D.H., and Maller, J.L. (1992). Periodic changes in phosphorylation of the *Xenopus* cdc25 phosphatase regulate its activity. *Mol. Biol. Cell* *3*, 927–939.
- Jacobs, D., Glossip, D., Xing, H., Muslin, A.J., and Kornfeld, K. (1999). Multiple docking sites on substrate proteins form a modular system that mediates recognition by ERK MAP kinase. *Genes Dev.* *13*, 163–175.
- Jones, S.W., Erikson, E., Blenis, J., Maller, J.L., and Erikson, R.L. (1988). A *Xenopus* ribosomal protein S6 kinase has two apparent kinase domains that are each similar to distinct protein kinases. *Proc. Natl. Acad. Sci. USA* *85*, 3377–3381.
- Kamps, M.P. (1991). Determination of phosphoamino acid composition by acid hydrolysis of protein blotted to Immobilon. *Methods Enzymol.* *201*, 21–27.
- Keyse, S.M. (1998). Protein phosphatases and the regulation of MAP kinase activity. *Semin. Cell Dev. Biol.* *9*, 143–152.
- Keyse, S.M., and Emslie, E.A. (1992). Oxidative stress and heat shock induce a human gene encoding a protein-tyrosine phosphatase. *Nature* *359*, 644–647.
- Kosako, H., Akamatsu, Y., Tsurushita, N., Lee, K.K., Gotoh, Y., and Nishida, E. (1996). Isolation and characterization of neutralizing single-chain antibodies against *Xenopus* mitogen-activated protein kinase kinase from phage display libraries. *Biochemistry* *35*, 13212–13221.
- Kosako, H., Gotoh, Y., Matsuda, S., Ishikawa, M., and Nishida, E. (1992). *Xenopus* MAP kinase activator is a serine/threonine/tyrosine kinase activated by threonine phosphorylation. *EMBO J.* *11*, 2903–2908.
- Kosako, H., Gotoh, Y., and Nishida, E. (1994a). Mitogen-activated protein kinase kinase is required for the mos-induced metaphase arrest. *J. Biol. Chem.* *269*, 28354–28358.
- Kosako, H., Gotoh, Y., and Nishida, E. (1994b). Requirement for the MAP kinase kinase/MAP kinase cascade in *Xenopus* oocyte maturation. *EMBO J.* *13*, 2131–2138.
- Kreegipuu, A., Blom, N., and Brunak, S. (1999). PhosphoBase, a database of phosphorylation sites: release 2.0. *Nucleic Acids Res.* *27*, 237–239.
- Kumagai, A., and Dunphy, W.G. (1996). Purification and molecular cloning of Plx1, a Cdc25-regulatory kinase from *Xenopus* egg extracts. *Science* *273*, 1377–1380.
- Lenormand, J.L., Dellinger, R.W., Knudsen, K.E., Subramani, S., and Donoghue, D.J. (1999). Speedy: a novel cell cycle regulator of the G2/M transition. *EMBO J.* *18*, 1869–1877.
- Lewis, T., Groom, L.A., Sneddon, A.A., Smythe, C., and Keyse, S.M. (1995). XCL100, an inducible nuclear MAP kinase phosphatase from *Xenopus laevis*: its role in MAP kinase inactivation in differentiated cells and its expression during early development. *J. Cell Sci.* *108*, 2885–2896.
- Lewis, T.S., Shapiro, P.S., and Ahn, N.G. (1998). Signal transduction through MAP kinase cascades. *Adv. Cancer Res.* *74*, 49–139.
- Lin, A.W., Barradas, M., Stone, J.C., van Aelst, L., Serrano, M., and Lowe, S.W. (1998). Premature senescence involving p53 and p16 is activated in response to constitutive MEK/MAPK mitogenic signaling. *Genes Dev.* *12*, 3008–3019.
- Mansour, S.J., Matten, W.T., Hermann, A.S., Candia, J.M., Rong, S., Fukasawa, K., Vande Woude, G.F., and Ahn, N.G. (1994). Transformation of mammalian cells by constitutively active MAP kinase kinase. *Science* *265*, 966–970.
- Matten, W.T., Copeland, T.D., Ahn, N.G., and Vande Woude, G.F. (1996). Positive feedback between MAP kinase and Mos during *Xenopus* oocyte maturation. *Dev. Biol.* *179*, 485–492.
- Meier, P., and Evan, G. (1998). Dying like flies [comment]. *Cell* *95*, 295–298.
- Minshull, J., Sun, H., Tonks, N.K., and Murray, A.W. (1994). A MAP kinase-dependent spindle assembly checkpoint in *Xenopus* egg extracts. *Cell* *79*, 475–486.
- Muda, M., et al. (1998). The mitogen-activated protein kinase phosphatase-3 N-terminal noncatalytic region is responsible for tight substrate binding and enzymatic specificity. *J. Biol. Chem.* *273*, 9323–9329.
- Pagès, G., Lenormand, P., L'Allemain, G., Chambard, J.-C., Meloche, S., and Pouyssegur, J. (1993). Mitogen-activated protein kinases p42mapk and p44mapk are required for fibroblast proliferation. *Proc. Natl. Acad. Sci. USA* *90*, 8319–8323.
- Palmer, A., Gavin, A.C., and Nebreda, A.R. (1998). A link between MAP kinase and p34^{cdc2}/cyclin B during oocyte maturation: p90^{rsk} phosphorylates and inactivates the p34^{cdc2} inhibitory kinase Myt1. *EMBO J.* *17*, 5037–5047.
- Payne, D.M., Rossomando, A.J., Martino, P., Erickson, A.K., Her, J.-H., Shabanowitz, J., Hunt, D.F., Weber, M.J., and Sturgill, T.W. (1991). Identification of the regulatory phosphorylation sites in pp42/mitogen-activated protein kinase (MAP kinase). *EMBO J.* *10*, 885–892.
- Pearson, G., Robinson, F., Beers Gibson, T., Xu, B.-E., Karandikar, M., Berman, K., and Cobb, M.H. (2001). Mitogen-activated protein (MAP) kinase pathways: regulation and physiological functions. *Endocr. Rev.* *22*, 153–183.

- Pfleger, C.M., and Kirschner, M.W. (2000). The KEN box: an APC recognition signal distinct from the D box targeted by Cdh1. *Genes Dev.* 14, 655–665.
- Posada, J., and Cooper, J.A. (1992). Requirements for phosphorylation of MAP kinase during meiosis in *Xenopus* oocytes. *Science* 255, 212–215.
- Robbins, D.J., Zhen, E., Owaki, H., Vanderbilt, C.A., Ebert, D., Geppert, T.D., and Cobb, M.H. (1993). Regulation and properties of extracellular signal-regulated protein kinases 1 and 2 in vitro. *J. Biol. Chem.* 268, 5097–5106.
- Rogers, S., Wells, R., and Rechsteiner, M. (1986). Amino acid sequences common to rapidly degraded proteins: the PEST hypothesis. *Science* 234, 364–368.
- Rohan, P.J., Davis, P., Moskaluk, C.A., Kearns, M., Krutzsch, H., Siebenlist, U., and Kelly, K. (1993). PAC-1: a mitogen-induced nuclear protein tyrosine phosphatase. *Science* 259, 1763–1766.
- Roy, L.M., Haccard, O., Izumi, T., Lattes, B.G., Lewellyn, A.L., and Maller, J.L. (1996). Mos proto-oncogene function during oocyte maturation in *Xenopus*. *Oncogene* 12, 2203–2211.
- Sagata, N., Oskarsson, M., Copeland, T., Brumbaugh, J., and Vande Woude, G.F. (1988). Function of c-mos proto-oncogene product in meiotic maturation in *Xenopus* oocytes. *Nature* 335, 519–525.
- Sagata, N., Watanabe, N., Vande Woude, G.F., and Ikawa, Y. (1989). The c-mos proto-oncogene product is a cytostatic factor responsible for meiotic arrest in vertebrate eggs. *Nature* 342, 512–518.
- Sambrook, J., Fritsch, E.F., and Maniatis, T. (1989). *Molecular Cloning: A Laboratory Manual*, 2nd ed., Cold Spring Harbor, NY: Cold Spring Harbor Laboratory.
- Sanger, F., Nicklen, S., and Coulson, A.R. (1977). DNA sequencing with chain-terminating inhibitors. *Proc. Natl. Acad. Sci. USA* 74, 5463–5467.
- Shaw, G., and Kamen, R. (1986). A conserved AU sequence from the 3' untranslated region of GM-CSF mRNA mediates selective mRNA degradation. *Cell* 46, 659–667.
- Slack, D.N., Seternes, O.M., Gabrielsen, M., and Keyse, S.M. (2001). Distinct binding determinants for ERK2/p38alpha and JNK map kinases mediate catalytic activation and substrate selectivity of map kinase phosphatase-1. *J. Biol. Chem.* 276, 16491–16500.
- Sohaskey, M.L., and Ferrell, J.E., Jr. (1999). Distinct, constitutively active MAPK phosphatases function in *Xenopus* oocytes: implications for p42 MAPK regulation in vivo. *Mol. Biol. Cell* 10, 3729–3743.
- Sun, H., Charles, C.H., Lau, L.F., and Tonks, N.K. (1993). MKP-1 (3CH134), an immediate early gene product, is a dual specificity phosphatase that dephosphorylates MAP kinase in vivo. *Cell* 75, 487–493.
- Sun, H., Tonks, N.K., and Bar-Sagi, D. (1994). Inhibition of Ras-induced DNA synthesis by expression of the phosphatase MKP-1. *Science* 266, 285–288.
- Wang, X.M., Zhai, Y., and Ferrell, J.E., Jr. (1997). A role for mitogen-activated protein kinase in the spindle assembly checkpoint in XTC cells. *J. Cell Biol.* 137, 433–443.
- Waskiewicz, A.J., and Cooper, J.A. (1995). Mitogen and stress response pathways: MAP kinase cascades and phosphatase regulation in mammals and yeast. *Curr. Opin. Cell Biol.* 7, 798–805.
- Wu, J., Michel, H., Rossomando, A., Haystead, T., Shabanowitz, J., Hunt, D.F., and Sturgill, T.W. (1992). Renaturation and partial peptide sequencing of mitogen-activated protein kinase (MAP kinase) activator from rabbit skeletal muscle. *Biochem. J.* 285, 701–705.
- Xia, Z., Dickens, M., Raingeaud, J., Davis, R.J., and Greenberg, M.E. (1995). Opposing effects of ERK and JNK-p38 MAP kinases on apoptosis. *Science* 270, 1326–1331.
- Yang, S.H., Whitmarsh, A.J., Davis, R.J., and Sharrocks, A.D. (1998a). Differential targeting of MAP kinases to the ETS-domain transcription factor Elk-1. *EMBO J.* 17, 1740–1749.
- Yang, S.H., Yates, P.R., Whitmarsh, A.J., Davis, R.J., and Sharrocks, A.D. (1998b). The Elk-1 ETS-domain transcription factor contains a mitogen-activated protein kinase targeting motif. *Mol. Cell. Biol.* 18, 710–720.
- Zhang, F., Strand, A., Robbins, D., Cobb, M.H., and Goldsmith, E.J. (1994). Atomic structure of the MAP kinase ERK2 at 2.3 Å resolution. *Nature* 367, 704–711.
- Zhou, G., Denu, J.M., Wu, L., and Dixon, J.E. (1994). The catalytic role of Cys124 in the dual specificity phosphatase VHR. *J. Biol. Chem.* 269, 28084–28090.
- Zhu, J., Woods, D., McMahon, M., and Bishop, J.M. (1998). Senescence of human fibroblasts induced by oncogenic Raf. *Genes Dev.* 12, 2997–3007.
- Zúñiga, A., Torres, J., Ubeda, J., and Pulido, R. (1999). Interaction of mitogen-activated protein kinases with the kinase interaction motif of the tyrosine phosphatase PTP-SL provides substrate specificity and retains ERK2 in the cytoplasm. *J. Biol. Chem.* 274, 21900–21907.